

## 1. Sensors

### TRULY CALORIMETRIC FLOW SENSOR CHIP BASED ON SURFACE CHANNEL TECHNOLOGY

*W. Sparreboom<sup>1\*</sup>, E.J. van der Wouden<sup>1</sup>, T.S.J. Lammerink<sup>2</sup>,  
and J.C. Lötters<sup>1,2</sup>*

<sup>1</sup> Bronkhorst High-Tech BV, Ruurlo, The Netherlands

<sup>2</sup> University of Twente, Transducers Science and Technology, Enschede, The Netherlands

#### ABSTRACT

In this paper we present a truly calorimetric flow sensor. The technology to fabricate the sensor is based on surface channel technology. The nominal measurable air flow is 0.8 ml<sub>n</sub>/min. The material of the sensor element is silicon nitride which is resistant to most commonly applied chemicals. The measurement tube is freely suspended and has a wall thickness of only 1 micron. This gives the tube an extremely low thermal mass which facilitates true calorimetric flow sensing. Calorimetric flow sensing allows for conversion between different gases based on their density and heat capacity product ( $\rho \cdot C_p$ ). This was checked experimentally for several common gases. Conversion between gases was found to be within 2%.

#### KEYWORDS

Thermal flow sensor, MEMS, Microfluidics

#### INTRODUCTION

Calorimetric flow sensors have the interesting property of  $\rho \cdot C_p$  conversion between gases. This facilitates calibration on a single gas (e.g. nitrogen) and conversion to other gases simply by  $\rho \cdot C_p$  for volumetric flow and  $C_p$  for mass flow. For decades these sensors have been manufactured mainly in steel. Since steel sensors typically have a relatively large thermal mass, these sensors have a response time typically higher than 1 s.

#### FLOW SENSOR DESCRIPTION

##### Novelty

Here we present a truly calorimetric MEMS gas flow sensor as opposed to semi calorimetric sensors introduced in literature before [1]. It has a nominal air flow of 0.8 ml<sub>n</sub>/min. It has a fast response time in the order of milliseconds and is chemically inert to most common gases.

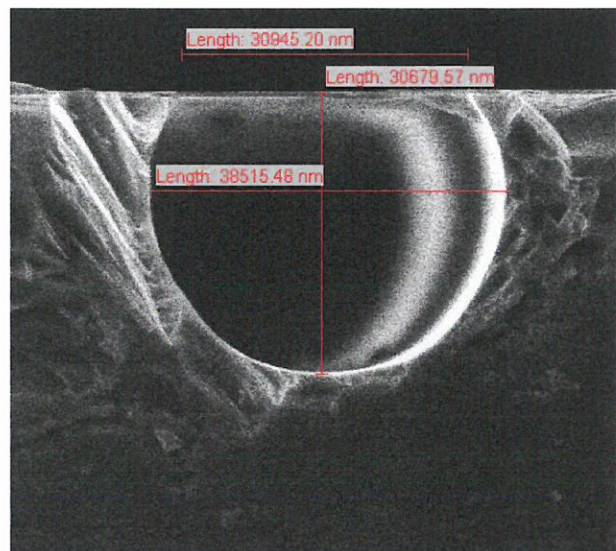


Figure 1: SEM picture of a surface channel fabricated by buried channel technology.

#### Chip

The sensor chip is based on the technology developed by Dijkstra et al [2]. With this technology buried channels can be fabricated. In figure 1 a scanning electron microscope (SEM) picture of a buried channel fabricated with this technology is given. A SEM picture of the functional part of the chip is depicted in figure 2. Here two tubes can be observed. The tubes are etched free from the substrate. Both tubes contain metal resistors that act as heaters and temperature sensors. Flow enters the tube in the bottom left of the picture via a surface channel inside the substrate. On the top right end of the picture a surface channel continuously (i.e. without steps in diameter) connects the two tubes. The free hanging tubes have an inner diameter of approximately 40  $\mu\text{m}$  and a wall thickness of approximately 1  $\mu\text{m}$ . Channels are fabricated using surface channel fabrication as described in [3,4]. The channel wall is silicon rich LPCVD silicon nitride. This material is chemically very resistive and allows for a broad range of applications. The material of the resistors is 200 nm



gold with 15 nm chromium for adhesion. They are sputtered on top of the nitride channels and are therefore galvanically separated from the medium.

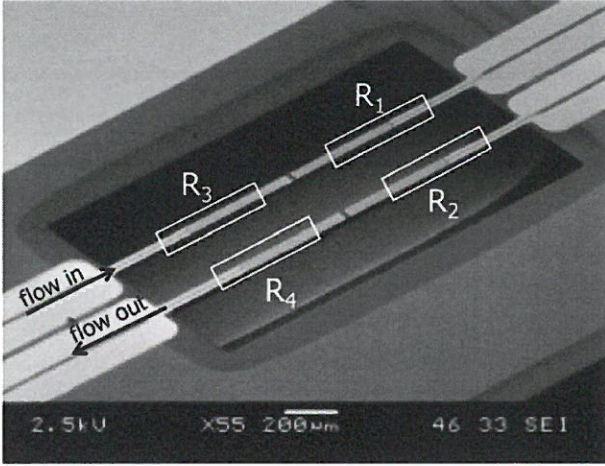


Figure 2: SEM picture of the chip with schematic representation of the gold resistors and the flow direction.

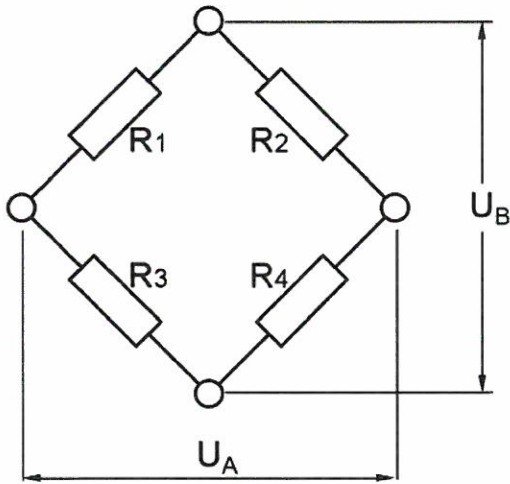


Figure 3: Heater / temperature sensor resistors in a Wheatstone bridge. The resistor numbers correspond to the definition in figure 2. A voltage is placed between  $U_B$ , the resulting voltage difference is measured at  $U_A$ .

### Electrical and fluidic interface

The chip has four temperature dependent resistors (figure 2) which are placed in a Wheatstone configuration (figure 3). A 100 mV potential is placed across the bridge ( $U_B$  in figure 3) using a digitally controlled voltage supply. The thus occurring electrical power heats up the resistors. If a flow is applied in the direction given in figure 2 a voltage difference occurs between the midsection of the left side and the right side branch of the bridge. This

voltage difference is a function of flow. It is measured in the midsection ( $U_A$  in figure 3) using a high impedance differential amplifier. The temperature dependent resistors have a DC value of approximately  $100 \Omega$  at  $T = 25^\circ\text{C}$ . The analog signals are digitized using a 24 bits analog to digital converter (ADC). This is then converted to an RS-232 signal in a microcontroller for communication with a computer.

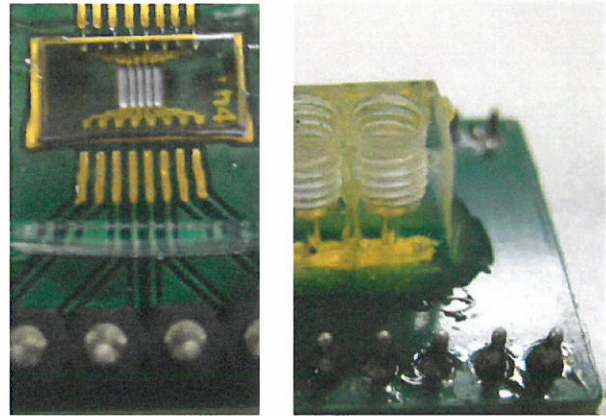


Figure 4: Left: Electrical chip interface. The chip looks distorted, because of an optical effect caused by the plastic cover. Right: Fluidic chip interface.

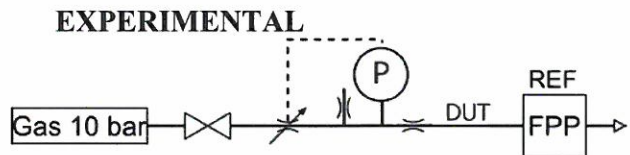


Figure 5: Schematic view of the setup. Gas pressure is delivered using a mechanical pressure controller at 10 bara. A pressure meter (P) is used to electronically control the pressure using an electromagnetic valve. Between the device under test (DUT) a restriction is placed and as a reference a 50 ml<sub>n</sub>/min piston prover (FPP) is used

The setup we used to characterize this system is given in figure 5. Gas flow is generated by an electronically controlled pressure at the inlet. We use a pressure controller for this (Bronkhorst, EL-PRESS) and a constant leak. The outlet is at atmospheric pressure which is also monitored during the experiment using a pressure sensor. As a volumetric flow reference we use a 50 ml<sub>n</sub>/min piston prover (Bronkhorst, FPP-050). Before the DUT (device under test) we placed a restriction (10 cm long stainless steel tube with an inner diameter of 125 μm). In this way the range of the pressure controller is more efficiently used. This in turn gives a higher resolution for the pressure control. We tested the sensor chip with 4 different gases, Argon (Ar), Helium (He), Nitrogen (N<sub>2</sub>) and Carbon dioxide (CO<sub>2</sub>).



## RESULTS

In this section we present and discuss the results obtained with the setup described above. We measured the resulting sensor signals as a function of the reference flow measured by the piston prover. An example of such a curve, measured with N<sub>2</sub> is given in figure 6.

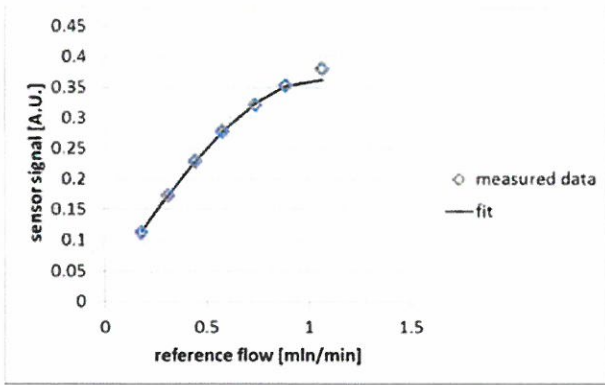


Figure 6. Measured sensor signal for N<sub>2</sub> as a function of reference flow by a 50 mln/min piston prover. The fit is a 3<sup>rd</sup> order odd function polynomial fitted by the least square method. The fit is reasonable up to approximately 0.8 ml<sub>n</sub>/min, which we define as its nominal flow rate.

We fitted the data with a third order odd function polynomial. This means we only used the first and third order term. This fit was found to describe the sensor signal most effectively. Later this polynomial function can also be applied to linearize the sensor response. The coefficient of the first order or linear part of the fit is used as the sensor sensitivity, S<sub>x</sub>, for a specific gas, x. If we plot this sensitivity as a function of ρ-C<sub>p</sub> for different gases we find a linear fit (figure 7). This is expected since we suppose S<sub>x</sub> is indeed a linear function of ρ-C<sub>p</sub>.

Moreover we find that Ar and He show similar sensitivities, which is expected since they have a similar ρ-C<sub>p</sub> product. To prove that the sensor sensitivity is a function of ρ-C<sub>p</sub> we define two types of conversion factors, a theoretical conversion factor TCF<sub>x</sub> and an empirical conversion factor ECF<sub>x</sub>. These are then used to directly compare the measured values with theory for each gas. In equation (1) TCF<sub>x</sub> is defined.

$$TCF_x = \frac{\rho_x C_{p,x}}{\rho_{N_2} C_{p,N_2}} \quad (1)$$

In TCF<sub>x</sub> the ratio of ρ-C<sub>p</sub> product of the gas of interest to the ρ-C<sub>p</sub> product of N<sub>2</sub> is determined. ECF<sub>x</sub> is defined in equation 2.

$$ECF_x = \frac{S_x}{S_{N_2}} \quad (2)$$

Here the ratio of the empirical sensitivity of the gas of interest and the empirical sensitivity of N<sub>2</sub> is determined. The theoretical and empirical conversion factors can be compared to determine the accuracy of conversion solely based on the ρ-C<sub>p</sub> product.

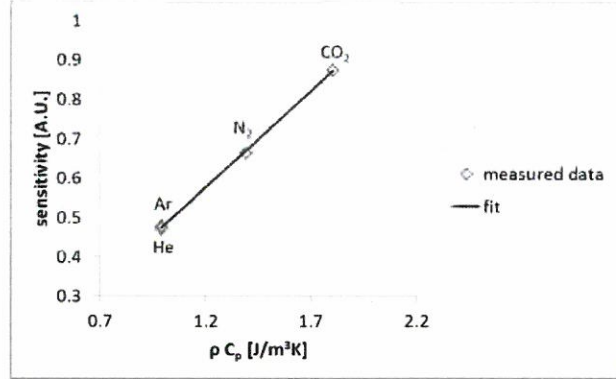


Figure 7. Measured sensitivity (slope of the linear part of the fit in figure 6) as a function of the theoretical ρ-C<sub>p</sub> product at 1.2 bar(a) and 30°C (average pressure and temperature inside the sensor).

In table 1 we show the conversion factors for different gases. Also the deviation between the theoretical and the empirical conversion factors is given. The deviation is well below 2% which is good enough for a proof of principle. Not only does this facilitate conversion between gases, it will also result in reproducible behavior between chips when applying gas mixtures that vary in composition during a measurement.

Table 1: Measured and theoretical conversion factors with respect to N<sub>2</sub>

	ECF <sub>x</sub> [measured]	TCF <sub>x</sub> [theoretical]	deviation [%]
He	0.707	0.711	-0.57
Ar	0.719	0.714	0.69
CO <sub>2</sub>	1.317	1.298	1.43

## CONCLUSION

To conclude we presented a truly calorimetric flow sensor chip. The sensor element is made of silicon nitride and the heaters are galvanically separated from the inner part of the sensor element. This makes the sensor chemically resistant to most gases. We tested this chip with several common gases and found predictable behavior. Moreover we found a

$\rho$ - $C_p$  relation between different gases. This eliminates the need for calibration with actual gases and opens up the road to measuring various mixtures reproducibly between sensor chips.

### ACKNOWLEDGEMENTS

This project was funded by MicroNed and Nanonext. We thank Jeroen Bos and Tristan Doornebosch for assistance with the gas measurements. Jarno Groenesteijn is thanked for assistance with the sensor connections and Lammert Heijnen for interesting and fruitful discussions.

### REFERENCES

[1] J.T.W. Kuo, L. Yu, E. Meng, "Micromachined Thermal Flow Sensors – A Review", *Micromachines*, 3 (2012), 550-573.

[2] M. Dijkstra, M.J. de Boer, J.W. Berenschot, T.S.J. Lammerink, R.J. Wiegerink, M. Elwenspoek, "A versatile surface channel concept for microfluidic applications", *J. Micromech. Microeng.*, 17 (2007) 1971-1977.

[3] M. Dijkstra, M.J. de Boer, J.W. Berenschot, T.S.J. Lammerink, R.J. Wiegerink, M. Elwenspoek, "Miniaturized thermal flow sensor with planar integrated sensor structures on semicircular surface channels", *Sensor. Actuat. A-Phys.*, 143 (2008) 1-6.

[4] T.S.J. Lammerink, J.C. Lötters, R.J. Wiegerink, J. Groenesteijn, J. Haneveld. "Single chip flow sensing system with a dynamic flow range of more than 4 decades", 16th International Solid-State Sensors, Actuators and Microsystems Conference, TRANSDUCERS 2011, 890-893 (2011).

### CONTACT

\*W. Sparreboom, [w.sparreboom@bronkhorst.com](mailto:w.sparreboom@bronkhorst.com)